CHARACTERIZATION OF THE WASTE ROCK AND PIT WALLS AT THE JUNDEE GOLD MINE SITE IN WESTERN AUSTRALIA AND IMPLICATIONS FOR LONG-TERM ISSUES[1].

Shannon Shaw[2], Jason Martin, Greg Meiers, Mike O'Kane, and Christoph Wels

Abstract. The Jundee mine site is an open pit and underground gold mine located 50 km northeast of the township of Wiluna in central Western Australia's desert. Jundee lies within the Archaean Yandal greenstone belt of the Western Australian goldfield. The area is deeply weathered and overlain by a thin veneer of alluvium and ferricrete. With the exception of satellite pits, open pit mining at Jundee ceased in 2002 and a number of open-cuts are being partially backfilled by waste rock, or tailings or left to flood with water. The primary sulfides in the waste rock and wall rock are pyrite and arsenopyrite. Carbonates are extensive on the site, consisting predominantly of calcite and ankerite. Given the rock types, mineralization and hydrothermal alteration of the waste rock, acid rock drainage is not anticipated; however, there is the potential for neutral drainage metal leaching and related water quality issues. Secondary mineral precipitates in localized areas include: hexahydrite, halite, gypsum, basanite, siderite and hematite. This paper describes the characterization program implemented, the results obtained and the implications for long- term issues at the site.

Additional Key Words: neutral drainage, metal leaching, salinity, hexahydrite, halite, siderite, basanite, gypsum, hematite.

_____

Introduction

The Newmont Jundee Operations (NJO) is located approximately 50 km northeast of the township and historic gold mines of Wiluna, approximately 750 km north-northeast of Perth in Western Australia. NJO consists of open pit and underground operations hosted in the Yandal belt of the western goldfields.

The climate at Jundee is arid with an average rainfall of 240 mm and an annual evaporation rate of 4,000 mm.

Open pit operations at NJO proper ceased in July 2002. There are a number of open pits on the site, some being partially backfilled by waste rock, or tailings and some being used for access/ventilation for the on-going underground operations of deeper orebodies. Figure 1 shows the open-cuts and the seven main waste rock dumps and two tailings storage facilities.
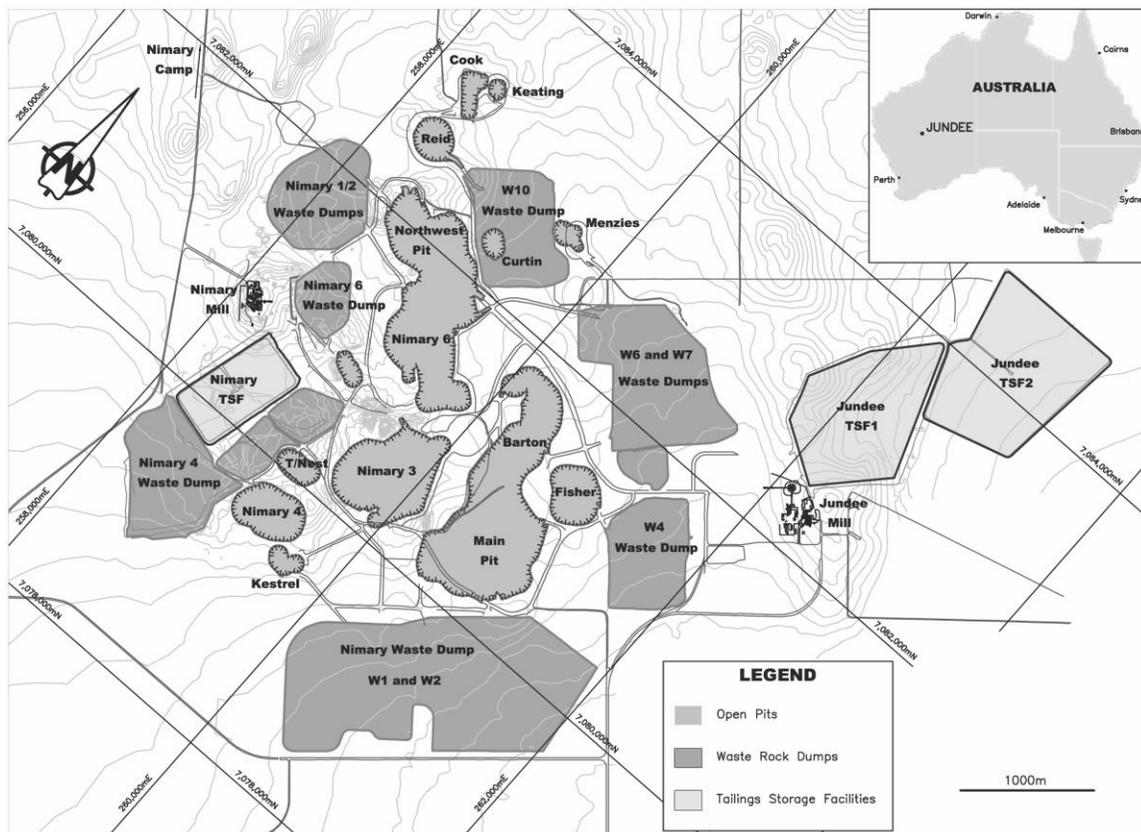
Figure 1. Location map and site plan.

Some rehabilitation measures have been conducted on a number of the waste dumps on site consisting primarily of encapsulation of 'higher' sulfidic material within oxide rock and placement of transitional and oxide waste on the outer slopes and upper surfaces. Some dumps have been contoured, ripped and revegetated.

Primary waste rock sourced from the open pits has also been used for a variety of purposes including armouring of dumps, partial backfilling of open pits and construction of infrastructure such as the ROM pads and tailings embankments.

This characterization study conducted and described in this paper was completed in order to describe and document the geochemical properties of the waste rock and pit wall rock on site, with focus on the primary rock, such potential issues or implications for long- term management of this material at the site could be identified and managed accordingly.

Geology

The NJO deposits are part of the Archaean Yandal greenstone belt in the northeast Yilgarn Craton of Western Australia, which hosts a number of Au deposits. The greenstone belt is dominated by mafic and ultramafic rocks, with a sequence of basalts and differentiated dolerites that are extensively intruded by dacites, granodiorites and lamprophyres, regionally metamorphosed to lower greenschist facies. In places, the mafic-ultramafic sequence contains units of black shale, dacitic volcaniclastic rock, and banded iron formation. The sequence is bounded to both the east and the west by Archaean granitoid-gneiss terranes.

The area is deeply weathered (~60 m), overlain by a thin veneer of alluvium and ferricrete rubble and in places, reworked and cemented lateritic material.

The entire thickness of the mine sequence is about 2.2 km and is dominated by two basalt units that contain massive and pillowed flows that are locally amygdaloidal and variolitic. Dacitic intrusives that are aphanitic to weakly porphyritic and grey-green in color with plagioclase (-hornblende-quartz), host significant primary Au mineralization in several of the deposits. Late stage porphyritic granodiorite dikes are also prevalent. The entire sequence has been metamorphosed to a greenschist facies assemblage with partial to complete replacement of primary pyroxene by actinolite and igneous plagioclase by albite (Kohler et al., 2001).

A deep regolith profile has developed over the crystalline rocks with complete oxidation generally observed in drill cuttings ranging in depths from 40 to 120 m. A combination of moderately bonded red mafic-rock-derived clay to poorly-bonded purple ashen clay, including highly oxidised relict silicified fragmental material, predominates throughout the oxide zone. A thin transitional zone of approximately 15m in thickness consists of partially oxidized, silicified material. Below the transitional zone, occasional isolated fractures with oxidised surfaces extend further into the basement or primary rock (IRC Environment, 2003).

In general, the Au ore occurs within shear-hosted quartz (-carbonate) veins and within the surrounding altered and strained wall rocks (including basalt, dolerite, dacitic volcaniclastics, carbonaceous shale and dacitic porphyry). The larger deposits on the site were developed in, or between, areas where two or more shear corridors intersect exhibiting strong structural control.

Hydrothermal alteration associated with Au mineralization is laterally zoned and overprints the metamorphic phases. The alteration zones are tangentially not extensive generally less than ~ 10m from the mineralization but can be up to 25m. A distal alteration zone is dominated by a chlorite-quartz-calcite alteration assemblage and the proximal alteration assemblage consists of a quartz-ankerite-calcite-muscovite-pyrite-arsenopyrite (-chlorite-rutile-leucoxene).

The primary sulfide is pyrite, with locally abundant arsenopyrite. Pyrite is typically disseminated euhedral to subhedral or composite grains with porous cores and eroded

boundaries. Arsenopyrite occurs as euhedral grains, or as inclusions and fracture infill in pyrite. Trace amounts of chalcopyrite, sphalerite, galena, pyrrhotite, tennantite-tetrahedrite, clausthalite, petzite, hessite, altaite and rarely tourmaline, chalcocite, digenite and covellite are also reported (Kohler et al., 2001).

Multi-element ICP analyses of the samples collected in this study compared closely to the crustal average basaltic to ultrabasic rock composition, with somewhat elevated levels of metals such as As, Cu, Co, Cr, Ni, S and Zn as would be expected in a mineralized region.

Water Quality

Groundwater quality monitoring data collected indicates some spatial variability in water quality. Most of the monitoring on site has focussed on the tailings storage facilities with the objective of monitoring water table mounding and any potential tailings and/or process water seepage from the storage facilities. No groundwater monitoring has been conducted around the waste dump facilities. Similarly, water quality data for groundwater associated with the open pits is limited. Salinity values reported in the groundwater data associated with the open pits from exploration drilling range from 3470 to 4510 mg/L (Phillips et al., 1998).

Water quality in one pit during a short monitoring period of approximately one year was alkaline (pH between 7.6 and 8) with elevated TDS values (8300 to 11,000 mg/L) and was dominated by Na, Cl$^-$ and SO$_4^{-2}$, with lesser amounts of Ca, Mg, HCO$_3^-$ and NO$_3^-$. Most metals were below detection limit, although As concentrations were marginally elevated (0.06 mg/L).

Geochemistry

A site reconnaissance trip and sampling program was initiated in order to document the current geochemical characteristics and potential for acid generation from the waste rock and pit walls on the site (Robertson GeoConsultants and O'Kane Consultants, 2005). This consisted of sampling of specific waste dump facilities, pit walls and run of mine (ROM) pads by surficial sampling and trenching means. Field measurements of paste pH and electrical conductivity (EC) were conducted and recorded and global positioning system (GPS) coordinates for all sample locations were mapped. Field notes were taken for each sampling location including descriptions of lithology, sulfide and carbonate mineralogy, colour, texture, grain size etc.

A total of 136 samples were collected for additional laboratory testing. This consisted of X-ray diffractometry (XRD), Paste pH and EC measurements (on the uncrushed, 'as-received' fines), Modified Acid Base Accounting (ABA), Multi-Element Inductively Coupled Plasma (ICP), Sequential Net Acid Generation (NAG), a modified EPA 1312 Leach Extraction (with Meteoric Water Mobility Procedure reagent), and Acid Base Characterisation Curves (ABCCs).

Field paste pH and EC measurements were taken on seeps and pit waters, where available, and on the 'fines fraction' (sieved to passing 4.76 mm) from samples of pit wall and waste rock. The results for the seep and pit pond water samples ranged in pH from 6.7 to 8.0 and EC values ranged from 5.3 to > 20 mS/cm (note 20 mS/cm is the upper limit of measurement for the field meters utilized). In general the pit seep and pond waters were well buffered with moderate to high conductivities and similar to the groundwater values available on record.

The field paste pH of solids material from the site ranged from 2.6 to 9.0 with an average value of 7.3 and a standard deviation of 1.2. Only 7 of the 136 samples (or ~ 5% of samples

tested) had paste pH values less than 5. These lower pH samples were primarily sourced from localized areas from the 3 specific dumps and 2 pits. The vast majority of material on site is well buffered to near neutral pH values. The EC measurements of material were more variable ranging from 0.1 to >20 mS/cm. Only 18 samples (or ~13% of material tested) had field paste EC values greater than 20 mS/cm. Paste EC measured on a subset of samples in the lab reported values up to 165 mS/cm.

The modified ABA analysis used here calculated MPA on the measured sulfide sulfur content and acid neutralizing capacity (ANC) as it is termed in Australia, or NP is measured as per the Sobek method (Sobek et al., 1978). Sulfide values ranged from 0.01% to 2.35% with an average of 0.17% and a standard deviation of 0.32%. Only 10 samples (~ 7% of material tested) reported sulfide sulfur values greater than 0.5%. The material that reported higher sulfide contents was sourced from one of the low-grade stockpiles, two of the pits, and two specific dumps.

Acid neutralisation capacity (ANC) values ranged from <1 to 360 kg $CaCO_3$/t equivalent. The average was calculated to be 63 kg $CaCO_3$/t equivalent with a standard deviation of 89 kg $CaCO_3$/t equivalent. The majority of samples reported relatively low ANC values; however 24% of the samples (33 samples) had ANC values greater than 100 kg $CaCO_3$/t equivalent. The samples with higher ANC values are all primary material, most often with carbonate veining evident and largely identified as basalt.

A plot of the MPA versus ANC is provided in Fig. 2. Also shown on the graph is the 2:1 ANC/MPA boundary used as an initial classification criterion for determining potentially acid forming (PAF) material versus non-acid forming (NAF). By and large, most of the material sampled plots well above this boundary in the NAF zone, a number of samples cluster right at the apex of the figure (i.e. have low ANC and MPA values) and a few plot well within the PAF field (with elevated MPA values and negligible ANC values). Of those that plot within the PAF field, the majority are from the two specific dumps and one stockpile that reported higher sulfide values. The ANC/MPA ratios ranged from 0 to over 1000 with an average of 35 and a standard deviation of 103. Twenty-five samples (~18%) reported ratios less than 2:1.

The Net Neutralization Potential (ANC minus MPA; or NNP) values for these samples ranged from –70 to 360 kg $CaCO_3$/t equivalent, with an average of 56 and a standard deviation of 87 kg $CaCO_3$/t equiv in the dataset (Robertson GeoConsultants and O'Kane Consultants, 2005). Fifteen samples or 11% of the dataset reported negative NNP values (or greater MPA than ANC).

For initial classification purposes at NJO, those samples with positive NNPs and/or ANC:MPA ratios greater than 2:1 were classified as NAF and those with negative NNPs and/or ANC:MPA ratios less than 2:1 were classified as PAF (Fig. 3).
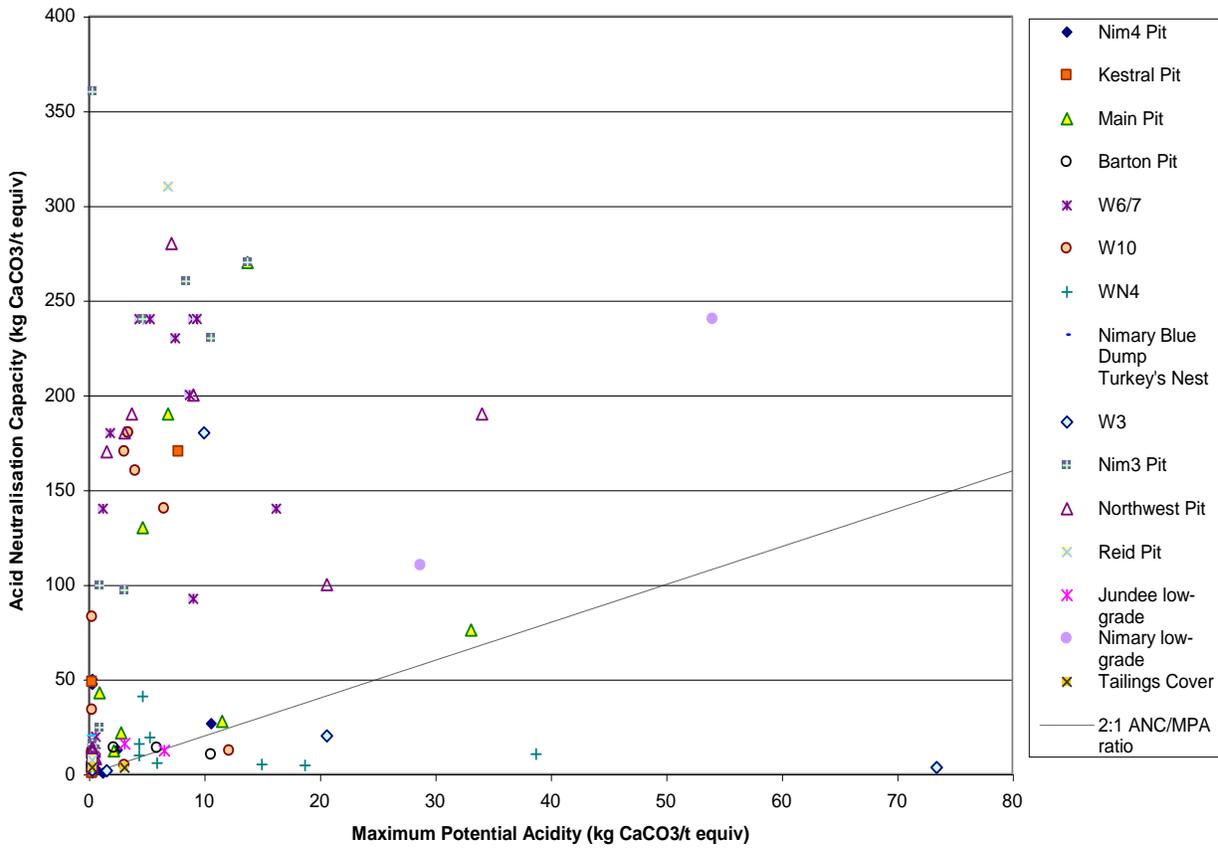
Figure 2. Maximum potential acidity (MPA) versus the acid neutralisation capacity (ANC). Refer to Fig. 1 for location of various dumps and pits.
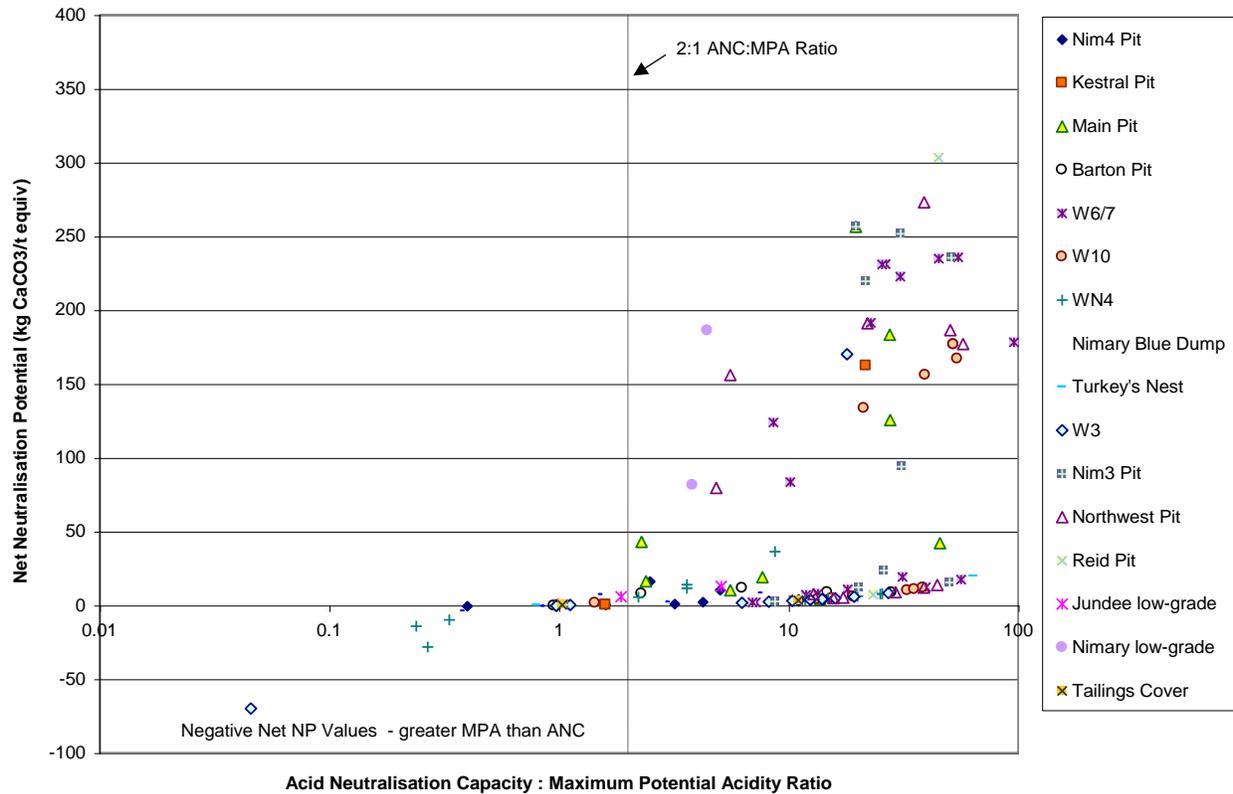
Figure 3. Ratio of acid neutralisation capacity (ANC) to maximum potential acidity (MPA) versus the net neutralisation potential (NNP). Symbols indicate different locations as shown on Fig. 1.

Sequential net acid generation (or NAG) tests were conducted on 5 samples, 4 of which confirmed the ABA classifications and one was in contradiction. The sample with contradicting classifications contained a secondary sulfate mineral (visually identified as jarosite), which may be a source of acidity in the NAG test but was not included in the MPA calculation of the ABA test. The dissolution of this mineral may be a source of acidity and metal leaching, in particular on pit walls during groundwater table rebound.

Acid Base Characteristic Curves (ABCCs) were also completed on six samples in order to assess the effectiveness of buffering at different pH conditions. The results are shown in Fig. 4. The samples chosen ranged in their ANC content from approximately 12 kg $CaCO_3$/t equivalent to 190 kg $CaCO_3$/t equivalent. The "effective" buffering capacity at different pH ranges can be assessed by comparing the ABCC results at a certain pH range to the ANC values. Table 1 shows the results of the measured ANCs and the effective ANC to a pH range between 4 and 5 as taken from the ABCC analyses (all in units of kg $CaCO_3$/t equivalent.). This pH range was chosen as a lower limit beyond which metal concentrations tend to increase considerably.

1967
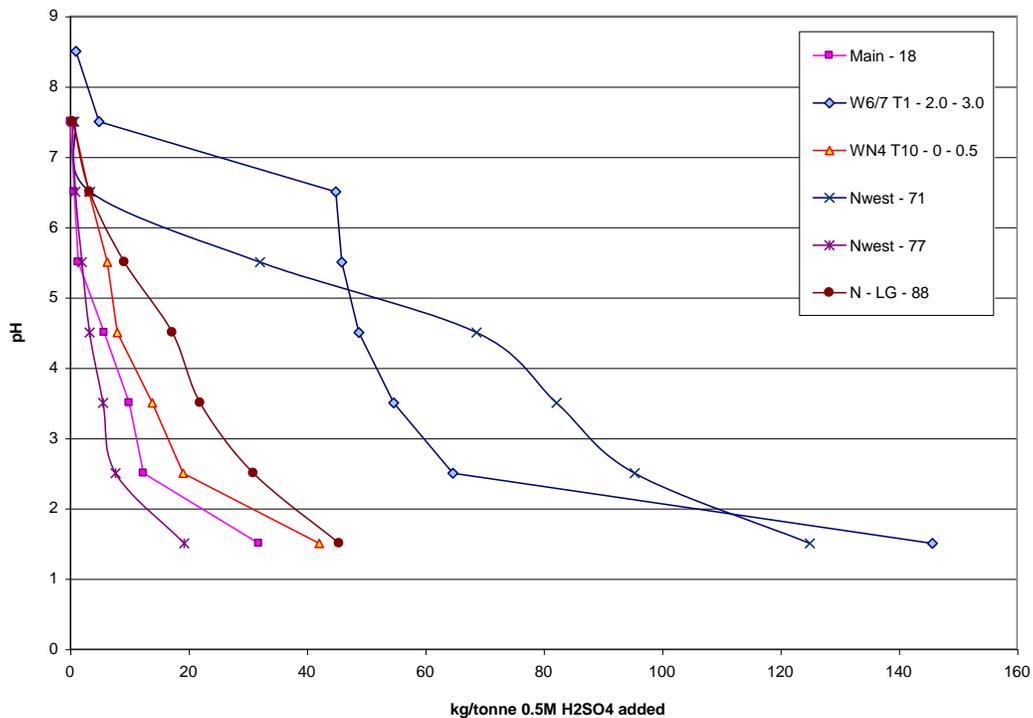
Figure 4. Acid base characteristic curves (ABCC) for six samples. Samples collected from Main and Northwest pits, W6/7 and WN4 dumps and Nimary lowgrade ROM pad as seen in Figure 1.

Table 1. ABA measured ANC compared to effective ANC based on ABCC evaluations.

Sample Type (Sample Label)	ABA Measured ANC (kg CaCO3/t equiv)	"Effective" ANC - ABCC to pH range 4 to 5 (kg CaCO3/t equiv)	Ratio of 'effective' ANC to measured ANC
Pit Wall (Main-18)	12	6	0.5
Waste Dump (W6/7 T1-2.0-3.0)	140	50	0.4
Waste Dump (WN4 T10-0-0.5)	16	8	0.5
Pit Wall (Nwest-71)	190	70	0.4
Pit Wall (Nwest-77)	12	3	0.3
ROM Pad (N-LG-88)	110	18	0.2

Using this pH range as a measure of "effective" ANC, it would suggest that roughly one fifth to one half of the measured ANC is actually effective at buffering the material above a pH range of 4 to 5.

Leach extraction tests were conducted on the samples using a reagent at pH 5.5 (to simulate meteoric water) and a solid to liquid ratio of 1:2. The resulting soluble content of each of the elements was calculated by comparing the leach extraction results with the multi-element ICP analyses. Constituents that are soluble to some extent in the material include B, Ca, K, Mg, Mn, Na, and SO_4^{-2} +/- As, Cd, Cr, Mo, Ni, Se and Zn. Based on the geology, it is anticipated that the Ca, Mg and possibly Mn are present largely as carbonates and as secondary minerals formed as a result of carbonate dissolution, and to a lesser extent from the dissolution of sulfates such as gypsum and the weathering of aluminosilicates such as feldspars. Similarly, B, K and Na are likely a result of aluminosilicate dissolution. The soluble SO_4^{-2} and metals are believed to be present as secondary minerals resulting from sulfide oxidation and dissolution. Secondary mineral phases, as suggested by the XRD analyses (see below) include, bassanite, halite, hexahydrite, ankerite, siderite, kieserite, anhydrite and gypsum, presumably as well as semi-crystalline to amorphous phases not detected by XRD analyses. Trace metals are likely to exist in these phases as impurities.

XRD analyses were conducted on seven samples selected with the above objectives in mind. These samples were largely collected near pit seeps or where evidence of seepage could be seen in the waste material. All samples were mixtures of primary and secondary minerals and were crushed in a McCrone micronizing mill to homogenize the samples and reduce particle size. Randomly oriented specimens were pressed onto Al holders. XRD patterns were recorded using a Philips PW1700 automatic diffractometer with X-rays generated from a Co x-ray tube operated at 40 kV and 30 mA diffracted by a graphite monochromator. Samples were scanned at 0.5^o per minute for a 2θ from 2° to 70°. Positions and intensities of diffraction patterns were calculated and compared to reference patterns.

Minerals identified by XRD consisted of albite $[(Na,Ca)Al(Si,Al)O_8]$, anyhdrite $[CaSO_4]$, ankerite $[Ca(Fe,Mg)(CO_3)_2]$, aragonite $[CaCO_3]$, bassanite $[CaSO_4.0.5H_2O]$, calcite $[CaCO_3]$, clinochlore $[(Mg,Fe)_6(Si,Al)_4O_{10}(OH)_2(Mg,Fe)_3(OH)_6]$, gypsum $[CaSO_4.2H_2O]$, halite $[NaCl]$, hematite $[Fe_2O_3]$, hexahydrite $[MgSO_4.6H_2O]$, kaolinite $[Al_2Si_2O_5(OH)_4]$, kieserite $[MgSO_4.H_2O]$, microcline $[KAlSi_3O_8]$, muscovite $[KAl_2(Si_3Al)O_{10}(OH,F)_2]$, quartz $[SiO_2]$, siderite $[FeCO_3]$.

The secondary minerals identified on many of the pit walls and at the toe of one dump where moisture contents were relatively high consisted of a mixture dominated by hexahydrite and halite. Figure 5 shows an example of this mixture that was identifiable by the white and bright green coloration. Leach extraction results on this material reported a leachate pH of 7.3 and soluble contents of particular parameters on the order of 1700 mg/kg S, 6 mg/kg Sr, 5300 mg/kg Na, 300 mg/kg K, 820 mg/kg Ca and 870 mg/kg Mg and negligible amounts of trace metals.

An unusual seep 'field' was evident on one particular dump in which black staining was seen on the dump face (Fig. 6) and along particular flowpaths in an excavated cut (Fig. 7). XRD analyses suggested that these precipitates were predominated by siderite and hematite. Leach extraction analyses of this material reported leach pH values of 6.4 and soluble amounts of major cations on the order of 2300 mg/kg Na, 100 mg/kg K, 430 mg/kg Ca and 3600 mg/kg Mg as well as trace metal contents of approximately 27 mg/kg Co, 3 mg/kg Ni, 2 mg/kg Se, 5 mg/kg Sn, 24 mg/kg Zn and 4400 mg/kg S.

Figure 5. Hexahydrite/halite 'salts' forming on pit wall near seep area.

Figure 6.   'Black' staining on surface of dump face consisting predominantly of siderite/hematite precipitates.

Figure 7. 'Black' staining as above on seep flowpaths as seen in dump cross-section.

Conclusions and Implications

The characterization included in this study indicates that there are only very minor, localized areas on the site that show depressed pH (i.e. acidity) and the potential for acid formation. The vast majority of material on site is not acidic and is considered to be non-acid forming.

There are, however, indications of neutral metal leaching in particular areas on site and electrical conductivity (salinity) indicating that there are stored soluble constituents in much of the material albeit largely non-acidic. Other visual signs of seepage were seen as a seep 'field' in one dump manifesting as dark brown to black seepage patches. Other seepage indicators occurred where moisture contents were higher such as at the toe of a particularly fine grained dump and near pit wall seeps (through fractures, cracks and drillholes) where secondary mineral crusts had formed. Secondary precipitates typically consisted of sulfate, chloride and carbonate precipitates (e.g. hexahydrite, halite and siderite) as well as oxides (hematite) as indicated by the XRD results. The primary constituents likely released from the secondary minerals on site during rainfall events would include Ca, Mg, Na, HCO_3^-, Cl and SO_4^{-2}. Soluble trace metals that exist in these phases as measured by leach extraction tests include As, Cd, Co, Cr, Mn, Mo, Ni, Se, Sn and Zn at relatively low levels. Of those parameters listed, only Cd, Co and Ni were elevated to levels above typical water quality guidelines in leach extraction tests.

It is recognized that the climate at Jundee is such that mobilization and transport of potential contaminants is limited. Occurrences of this type of seepage may continue to manifest themselves as seep stains that travel limited distances before precipitating as is currently seen in

the seep 'field' described herein. The most likely implication of this type of seepage is salinity increases and the potential for impact to revegetation efforts in these localized areas.

Within the pits themselves, much of the backfill material and primary pit wall rock sampled in this study contains substantial neutralization capacity in the form of carbonate veining. It is expected that these materials will add net alkalinity to the pit systems. It has been the assessment of hydrogeological work conducted by others that there will remain a cone of depression towards the open pits and underground workings post mining. As such, there is little anticipated risk to regional groundwater from interactions with pit water qualities as the water will remain 'trapped' in the local depression or 'hydraulic cage'. The groundwater table will however likely rebound to some level resulting in standing water in the open pits. The water quality in these 'lakes' will be dependent on a number of factors:

- The water quality and rate of the rebounding groundwater,

- Interactions of the rising water with the pit walls,

- Precipitation and run-on (over exposed pit walls),

- Solubility constraints due to secondary mineral precipitation, and

- Evaporation (and evapo-concentration).

Best estimates of pit water quality are qualitative to date, but suggest a slightly alkaline, saline pit lake with elevated TDS values dominated by Na, Cl^- and SO_4^{-2}, with lesser amounts of Ca, Mg, HCO_3^- and NO_3^- and negligible metals with the possible exception of Cd, Co and Ni +/- As.

Evaporation is anticipated to play a fairly dominant role in the chemistry within the pit lake system given the climate at Jundee. This will likely result in gradual increases in concentration of the constituents within the lake system and potentially the development of a density stratified lake 'trapping' the poorer water quality at depths in the form of a stratified hydraulic cage post closure.

Literature Cited

IRC Environment (2003). Seepage Investigations at Jundee and Nimary Tailings Storage Facilities, Report prepared for Newmont Australia, Sept 4, 2003, Doc No. ENV-REP-J03-090-001 REV 0

Kohler, E., Gebre-Mariam, M., Maclean, D., Yeats, C., Gass, S., Preston, P., Hall, D., Bryant, P., Everitt, M. and Biggam, J. (2001). Archaean lode-gold mineralization at Jundee-Nimary, north Yandal greenstone belt, Yilgarn Craton, Western Australia, pp. 197-216.

Phillips, G.N., Vearncombe, J.F. and Murphy, R. (1998). Jundee gold deposits. In Geology of Australian and Papua New Guinean Mineral Deposits (Eds: D.A Berkman and D.H. Mackenzie), pp. 97-104 (The Australasian Institute of Mining and Metallurgy: Melbourne).

Robertson GeoConsultants Inc. and O'Kane Consultants Pty. (2005). Waste Rock Characterisation and Implications for Long-Term Void Water Quality, Newmont Jundee Operations, Western Australia. OKC Report No. 686/4 prepared for Newmont Jundee Operations, September 2005.

Sobek, A., W. Schuller, J. Freeman, and R. Smith. 1978. Field and laboratory methods applicable to overburdens and minesoils. EPA-600/2-78-054. U.S. Environmental Protection Agency, Cincinnati, OH.

USGS (2005). PHREEQC Interactive, Version 2.11.0.148, Implements PHREEQC 2.11, released Feb 7, 2005.